Synthesis of coordination polymers based on a 2,2'-dimethoxy-1,1'-biphenyl scaffold and Hg(II), Co(II), or Zn(II)

El Mostafa Ketatni, Nathalie Kyritsakas, Pierre Mobian, Abdelaziz Jouaiti

Synthesis of coordination polymers based on a 2,2'-dimethoxy-1,1'-biphenyl scaffold and Hg(II), Co(II), or Zn(II)

El Mostafa Ketatni[b], Nathalie Kyritsakas[a], Pierre Mobian[a]*, Abdelaziz Jouaiti[a]*

[a]CNRS, CMC UMR 7140, Université de Strasbourg, 4 rue Blaise Pascal, F-67000, Strasbourg, France.
[b]Laboratory of Organic and Analytical Chemistry, University Sultan Moulay Slimane, Faculty of Science and Technology, B.P.523, 23000, Beni-Mellal, Morocco

*Correspondence e-mail address: jouaiti@unistra.fr, mobian@unistra.fr

Abstract

In this study, 3,3'-di(pyridin-4-yl)-(2,2'-dimethoxy-[1,1'-biphenyl]) (**L**) was synthetized, structurally characterized by X-ray crystallography and combined with $HgCl_2$, $CoCl_2$, or $ZnSiF_6$ for the formation of three coordination polymers ($(HgCl_2)_2(\boldsymbol{L})$, $(CoCl_2)_2(\boldsymbol{L})_2.CHCl_3$, and $Zn(SiF_6)(\boldsymbol{L})_2$). The crystal structures of synthesis compound indicate the formation of different types of coordination modes, and each adopts a mono (1D) or tri-dimensional (3D) framework by C–H$\cdots\pi$ interactions. In $(CoCl_2)_2(\boldsymbol{L})_2$, the combination of Co(II) with **L** forms a metallo-macrocycle, while in the other compounds two helical infinite networks were characterized. Compounds $(HgCl_2)_2(\boldsymbol{L})$ made of two helical chains with opposite chirality (*P* and *M*), and $Zn(SiF_6)(\boldsymbol{L})_2$ exhibits helical tubular assemblies of the **L** attached to two $Zn(SiF_6)_\infty$ pillars. This work may pave the way to further study the chemical, structural and physicochemical properties of metal-organic coordination polymers.

Keywords: Coordination polymers, 2,2'-dimethoxy-1,1'-biphenyl, Pyridine, Helical networks.

,

1. Introduction

Helicity is ubiquitous in Nature as many biological helical polymers (e.g, DNA) play fundamental but critical roles in various essential cellular functions [1]. Thus, inspired by these biomolecules, great efforts have been devoted to create synthetic helical molecules, polymers, organic assemblies, or coordination polymers (CPs) [2-5]. Coordination polymers also referred to as metal-organic coordination networks include a large family of compounds formed by central metal ions linked to several ligands by coordination bonds. It is an infinite extension driven by a self-assembly process into one (1D), two (2D), or three dimensions (3D) [6-11]. The design and synthesis of CPs have attracted much attention over the last decades due to the porosities, the great structural varieties and, more importantly, the potential for innovative applications in catalysis, gas storage, luminescence, and sensing, and other similar arenas [12–20]. Thereby, several coordination polymers have been synthesized. However, to obtain CPs with desirable properties and reactivity, appropriate organic ligands and metal ions must be judiciously selected [21–23].

In a previous article, we reported the synthesis of three-dimensional (3D) helical chiral framework by combining the 2,2'-dimethoxy-1,1'-biphenyl backbone and Silver salts [24]. In these systems, the helicity of the resulting networks is clearly arising from the twisted arrangement of the two phenyl rings within the starting ligand. The non-coplanarity of the two aromatic rings, which is essential to generate helicity at the metallosupramolecular level, is caused by the presence of substituents at the *ortho* positions to the C-C biphenyl junction.

Based on this elegant works mentioned above and the interest of our research group [25, 26], we designed and synthesized 3,3'-di(pyridin-4-yl)-(2,2'-dimethoxy-[1,1'-biphenyl]) (***L***) (Fig. 1) by Suzuki-Miyaura coupling reaction between 2,2'-dimethoxy-1,1'-biphenyl-3,3'-bisboronic acid and 4-bromopyridine. Therefore, we associate ***L*** with the three metal salts (Hg, Co, and Zn) and generate a novel coordination polymer $(HgCl_2)_2(\boldsymbol{L})$, $(CoCl_2)_2(\boldsymbol{L})_2.CHCl_3$, and $Zn(SiF_6)(\boldsymbol{L})_2$ under mild reaction condition. They were characterized by single-crystal X-ray diffraction. The combined results of this study revealed the significant effect of the three metal ions on the structural topology of the resulting polymers.

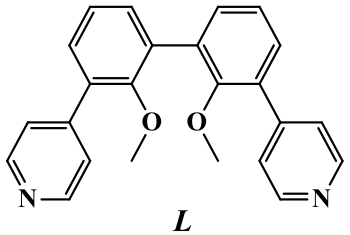

L

Figure 1: Molecular structure of 3,3'-di(pyridin-4-yl)-(2,2'-dimethoxy-[1,1'-biphenyl]) (***L***)

2. Experimental

2.1. Materials and methods

The starting materials and solvents were purchased from commercial suppliers and used without further purification. ^{1}H- and ^{13}C NMR spectra were recorded at 298 K on either Bruker AV300 or Bruker AV500 spectrometers in deuterated solvents, and the residual solvent peak was used as the internal reference. All the chemical shifts (δ) are reported in ppm. Elemental analyses were performed by the Service de Microanalyses de la Fédération de Recherche Chimie, Université *de Strasbourg*, Strasbourg, France.

2.2. Synthesis

2.2.1. Synthesis of 3,3'-di(pyridin-4-yl)-(2,2'-dimethoxy-[1,1'-biphenyl]) (*L*)

The reaction was conducted under a nitrogen atmosphere. A toluene solution (90 mL) of 4-bromopyridinium chloride (3.8 g, 19.95 mmol) was placed in a 250 mL two-neck round bottom flask then stirred, degassed. $Pd(PPh_3)_4$ (3.6 mol%) was successfully added and a degassed aqueous solution of Na_2CO_3 (15 mL, 1M) was transferred *via* cannula to the mixture. Afterward, a degassed solution of 2,2'-dimethoxy-1,1'-biphenyl-3,3'-bisboronic acid [27] (2g, 6.64 mmol) in 30 mL of methanol was transferred via cannula to the mixture. The resulting solution was stirred and heated at 120°C for 24 hours. Upon six hours of heating, $Pd(PPh_3)_4$ (1.4 mol%) was added to the reaction. The solution was allowed to warm up to room temperature and then washed with water (150 mL) and dichloromethane (2 ×150 mL). The organic layer was washed two more times with water (150 mL), dried over $MgSO_4$, and evaporated under a vacuum. The crude material was purified over alumina gel chromatography (CH_2Cl_2/MeOH, 99/1) to yield a white crystalline solid (67 %).

^{1}H NMR (300MHz, $CDCl_3$): δ (ppm) 8.68- 8.66 (dd, ^{3}J = 4.6 Hz, ^{4}J = 1.5 Hz, 4H), 7.58-7.56 (dd, ^{3}J = 4.4 Hz, ^{4}J = 1.6 Hz, 4H), 7.45-7.39 (dd, ^{3}J = 7.7 Hz, ^{4}J = 1.8 Hz, 4H), 7.31-7.26 (dd, ^{3}J = 7.5 Hz, 2H), 3.26 (s, 6H). ^{13}C NMR (75MHz, CD_2Cl_2): δ (ppm) 155.5, 149.7, 146.3, 132.7,

132.4, 132.1, 130.3, 124.0, 123.9, 60.7. IR (KBr, cm^{-1}): 3025, 2997, 2936, 2885, 2826, 1598, 1454, 1403, 1227, 1002. UV-Vis: $\log(\varepsilon_{272})$= 3.06 $L.mol^{-1}cm^{-1}$. Mp: 185°C. Elem. Anal. Calcd for $C_{24}H_{20}N_2O_2.1/2H_2O$: C, 76.17; H, 5.86; N, 7.40. Exp: C, 76.17; H, 5.43; N, 7.30. ESI-MS: m/z found, 369.394 ([**L**+H^+]); calcd, 368.394 ([**L**]). X-ray analysis CCDC n° 2064620.

2.2.2. Crystallization conditions

Chloroform solution (2 mL) of the ligand ***L*** (3 mg) was placed in a tube (height = 6.5 cm, diameter 0.4 cm); then, slowly layered over metal salt ($HgCl_2$, $CoCl_2$, or $ZnSiF_6$, respectively) (4 mg) solution in EtOH (3 mL). Solution tube was sealed and left allowed to stand at room temperature, upon slow diffusion at room temperature~~.~~ The colorless crystals suitable for X-ray analysis were obtained after a few days. Unfortunately, the microanalysis or powder diffraction pattern has not been provided due to the instability and collapse of crystals ($(HgCl_2)_2$(***L***), $(CoCl_2)_2$(***L***) $_2$.CHCl3, and $Zn(SiF_6)$(***L***)$_2$) upon removal of solvent molecules.

2.3. Crystal X-ray data collection and refinement

Single-crystal X-ray diffraction data for title compound were collected on a ~~A~~ Bruker APEX-II CCD crystal X-ray diffractometer with Mo-Kα radiation (λ = 0.71073 Å) monochromated by graphite at 173K. The Frame were integration with the Bruker SAINT Software package using a wide-frame algorithm., ~~and~~ Data were corrected for absorption by the multi-scan semi-empirical method implanted in SADABS [28]. The crystal structure was solved by direct methods using SHELXTL- 2014/5 [29] and refined by weighted full matrix least-squares on F^2 using SHELXL-2018/3 program [30]. All non-hydrogen atoms were assigned–anisotropic thermal parameters in the refinement. The C-bound H atoms were geometrically placed (C—H = 0.95 – 0.99 Å) and refined as riding with *U*iso(H) = 1.2 – 1.5 *U*eq(C). The N/O-bound H atom was located in a different Fourier map and refined freely. Crystal data, data collection, and structure refinement details for $(HgCl_2)_2$(***L***)**,** $(CoCl_2)_2$(***L***)$_2$.$CHCl_3$, and $Zn(SiF_6)$(***L***)$_2$) were summarized in Table 2. The plot of the molecule and the three-dimensional drawing of the crystal structure are obtained using the Diamond programs (Figures 2-5) [31] and Mercury CCDC (Figure 6).

3. Results and discussion

3.1. Synthesis

The ligand ***L*** (Scheme 1.) was synthesis by Suzuki -Miyaura coupling reactions between 2,2'-dimethoxy-1,1'-biphenyl-3,3'-bisboronic acid [27] and 4-bromopyridine in the presence of

Pd(0), which was obtained as two 4-pyridyl units in good overall yield (67%). Colorless crystals (67%) were obtained by slow diffusion of *n*-pentane into a CH_2Cl_2 solution of ***L***.

The coordination polymer networks were synthesized under mild reaction condition. A solution of $HgCl_2$, $CoCl_2$, or $ZnSiF_6$ in EtOH was carefully layered on a solution of ***L*** in $CHCl_3$. After three days, colorless crystals of the $(HgCl_2)_2$(***L***)**,** $(CoCl_2)_2$(***L***)$_2$.$CHCl_3$, and $Zn(SiF_6)$(***L***)$_2$ suitable forsingle-crystal X-ray diffraction were collected, respectively.

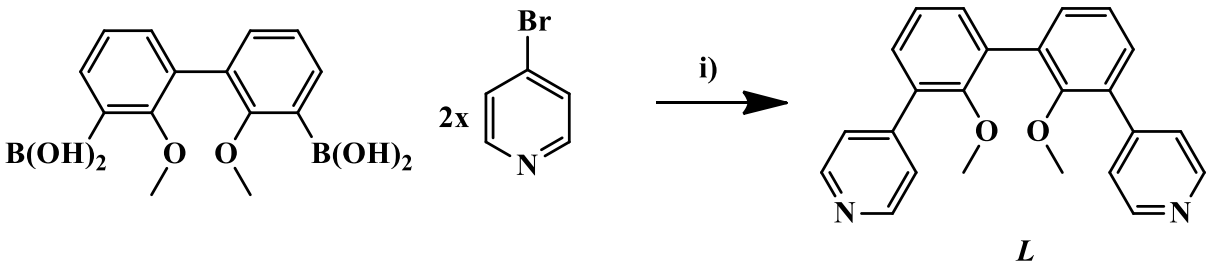

Scheme 1. Synthesis of ***L***. Reagents and conditions: i) Toluene/Methanol/H_2O 6/2/1, Na_2CO_3, $Pd(PPh_3)_4$, 120°C, 24 h

3.2. Crystal structure of the ligand *L*.

The single-crystal X-ray diffraction studies (Fig. 2) reveals that ***L*** crystallizes in the centrosymmetric triclinic group space $P\bar{1}$ and its asymmetric unit is comprised of a fully occupied ligand (Fig. 2a, Table 1).

Selected bond lengths and angles for the ligand **L** are listed in Table 2. The dihedral angle between the mean planes of the pyridine ring is calculated to be 82.36(8)°, which indicates the molecule is not planar. The mean planes of the N1/C1-C5 and C6-C11 make an angle of 59.02(7)°, while the N2/C20-C24 and C13-C18 rings make an angle of 41.02(7)°. Therefore, the mean planes of the benzene ring C6-C11 and C13-C18 is nearly perpendicular with a dihedral angle of 86.33(7)°.

In crystal **(*L*)**, molecules are linked by pairs of C—H···N hydrogen bonds interactions, forming centrosymmetric dimers with an $R_2^2(26)$ ring motif (Fig.2b and Table 2). These dimers are connected by C—H···π interactions to create a layer parallel to the bcplane (Fig. 2c, Table 3).

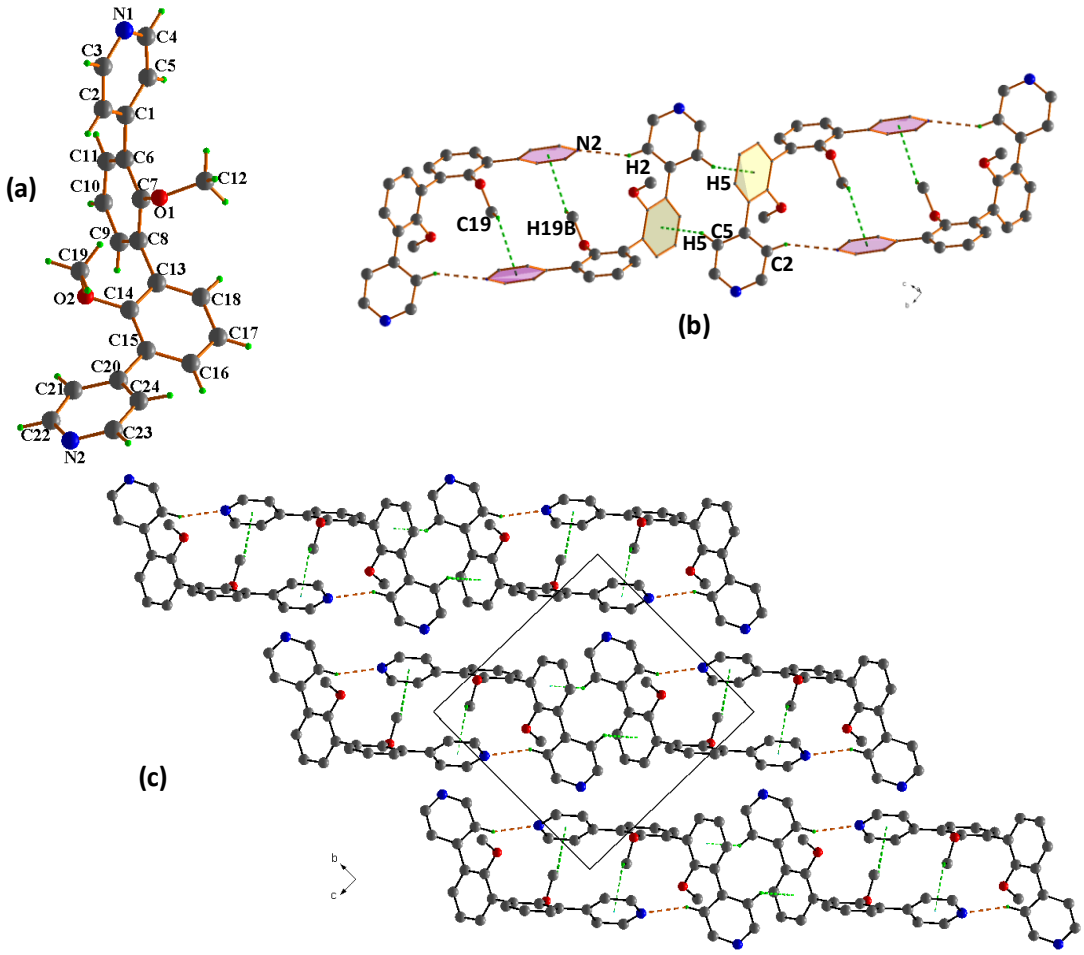

Figure 2: (a) The asymmetric unit of **(*L*)** showing the atom numbering scheme, (b) supramolecular architecture showing C—H···N hydrogen bond interactions and C—H···π interactions and (c) crystal packing.

Table 1: Crystal Data, Summary of Intensity Data Collection, and Structure Refinement

Cif	**S1673**	**S2031**	**S1754**	**S1755**
Chemical formula	$C_{24}H_{20}N_2O_2$	$(CoCl_2)_2(\boldsymbol{L})_2.CHCl_3$	$(HgCl_2)_2(\boldsymbol{L})$	$Zn(SiF_6)(\boldsymbol{L})_2$
M_r	340.37	1115.87	911.40	944.30
Crystal system, space group	Triclinic, $P\bar{1}$	Monoclinic, *C*2/c	Orthorhombic, *P*bca	Orthorhombic, *C*222
Temperature (K)	173(2)	173(2)	173(2)	173(2)
a, *b*, *c* (Å)	7.1212(7),11.4029(10),11.8997(12)	16.2412(10), 12.6402(8), 24.7617(17),	25.0073(4), 8.2559(1), 27.0784(4)	15.0501(6), 27.7485(12), 14.8660(6)
α, β, γ (°)	88.666(3), 79.221(3), 88.491(3)	102.207(2)	90, 90, 90	90, 90, 90
V (Å^3)	948.74(16)	4968.4(6)	5590.5(2)	6208.3(4)
Z	2	4	8	4
Radiation type	Mo *K*α	Mo *K*α	Mo *K*α	Mo *K*α
μ (mm^{-1})	0.08	1.09	11.38	0.47
Crystal shape and color	Prism, colorless	Prism, colorless	Prism, colorless	Prism, colorless
Crystal size (mm)	0.14 × 0.10× 0.10	0.05 × 0.04× 0.009	0.10 × 0.06× 0.05	0.08x0.06x0.05
Limiting indices	-9 ≤h ≤7, -12 ≤ k ≤14, -15 ≤ l ≤15	-22 ≤h ≤17, -17 ≤ k ≤12, -34 ≤ l ≤34	-33 ≤h ≤35, -11 ≤ k ≤7, -37 ≤ l ≤38	-19≤h ≤19, 0 ≤ k ≤36, 0 ≤ l ≤19
Diffractometer	Bruker APEX-II CCD	Bruker APEX-II CCD	Bruker APEX-II CCD	Bruker APEX-II CCD
Absorption correction	Multi-scan *(SADABS)*	Multi-scan *(SADABS)*	Multi-scan *(SADABS)*	Multi-scan *(SADABS)*
T_{min}, T_{max}	0.981, 0.996	0.940, 0.998	0.385, 0.650	0.956, 0.987
No. of measured, dependent and observed [$I > (I)$] reflections	12700, 4091, 3711	22986, 7208, 6124	74457, 8178, 6122	7153, 7153, 6027
R_{int}	0.020	0.029	0.049	0.054

Refinement method	Full-matrix least-squares on F^2	Full-matrix least-squares on F^2	Full-matrix least-squares on F^2	Full-matrix least-squares on F^2
$R[F^2 > 2s(F^2)]$, $wR(F^2, S$	0.043, 0.124, 1.01	0.047, 0.125, 1.05	0.026, 0.052, 1.05	0.047, 0.153, 1.07
Data/restraints/parameters	4091/0/255	7208/0/318	8178/0/328	71530/293
H-atom treatment	H-atom parameters constrained	H-atom parameters constrained	H-atom parameters constrained	H-atom parameters constrained
$\Delta\rho_{max}$, $\Delta\rho_{min}$ (e Å^{-3})	0.22, -0.19	0.57, -0.54	1.37, -0.88	1.04, -0.43
Absolute structure	-----	-----	-----	Flack x determined using 2389 quotients [(I+)-(I-)]/[(I+)+(I-)] (Parsons, Flack and Wagner, Acta Cryst. B69 (2013) 249-259).
Absolute structure parameter	-----	-----	-----	0.004 (19)

Table 2: Selected experimental geometrical parameters (Å, °) of ***L***

L			
C3—N1	1.338(2)	C22—N2	1.340(2)
C4—N1	1.329(2)	C23—N2	1.333(2)
C7—O1	1.385 (2)	C14—O2	1.380 (2)
C12—O1	1.433 (2)	C19—O2	1.434 (2)
C3—N1—C4	116.3 (2)	C22—N2—C23	115.9 (2)
N1—C3—C2	124.1(2)	N2—C22—C21	124.3(2)
N1—C4—C5	124.3(2)	N2—C23—C24	124.0(2)
C7—O1—C12	114.1(2)	C14—O2—C19	113.8(2)
O1—C7—C6	119.9 (2)	O2—C14—C13	118.4 (2)
O1—C7—C8	119.1(2)	O2—C14—C15	120.5(2)

Table 3: Hydrogen bonds interactions (Å, °) for ligand, complex $(CoCl_2)_2(\boldsymbol{L})_2.CHCl_3$, and $Zn(SiF_6)(\boldsymbol{L})_2$, Cg3 and Cg4 represent the centroid of the C6–C11 and C18–C23 rings.

	D—H···A	**D—H**	**H···A**	**D···A**	**D—H···A**	***Symmetry codes***
L	C2—H2···N2	0.95	2.55	3.414(2)	152	-x, -y, -z
	C5—H5···Cg2	0.95	2.81	3.561(2)	137	-x, 1-y, 1-z
	C19—H19B···Cg3	0.98	2.98	3.658(2)	128	-x, -y, -z
$(CoCl_2)_2(\boldsymbol{L})_2$	C5—H5···Cl1	0.95	2.81	3.497(2)	130	1/2-x,-1/2+y,1/2-z
	C1—H1···Cl2	0.95	2.79	3.357(2)	119	1/2-x,1/2+y,1/2-z
	C25—H25···O1	1.00	2.56	3.193(7)	121	x, 1-y, ½+z
	C25—H25···O2	1.00	2.56	3.480(7)	154	x, 1-y, ½+z
	C18—H18···Cl2	0.95	2.81	3.754(2)	173	1-x, y,1/2-z
	C19—H19B···Cg3	0.98	2.78	3.486(3)	139	1-x, 1-y, -z
$Zn(SiF_6)(\boldsymbol{L})_2$	C2—H2···O2	0.95	2.38	3.310(5)	166	2-x,y,1-z
	C5—H5···F1	0.95	2.52	3.058(5)	116	3/2-x,3/2-y,z
	C14—H14···O1	0.95	2.29	3.122(6)	145	2-x,y,1-z
	C17—H17···F3	0.95	2.43	3.363(5)	166	-1/2+x,3/2-y,1-z
	C9—H9···Cg4	0.95	2.73	3.599(6)	152	x,2-y,1-z
	C21—H21···Cg3	0.95	2.78	3.599(5)	144	x,y,1+z

3.3. Crystal structure of $(HgCl_2)_2(\boldsymbol{L})$.

The complex $(HgCl_2)_2(\boldsymbol{L})$ crystallizes in the orthorhombic crystal system with space group *P*bca (Table 1). The significant bond lengths and bond angles are provided in Table 4. The title compound is a one-dimensional coordination polymer consisting of $HgCl_2$ units joined by a bridging ligand (Fig. 3a). The Hg^{II} ion is tetracoordinated by three chloride ligands and one N atom of the bridging ligands forming a distorted tetrahedron. For both Hg1 and Hg2, the coordination is characterized by three short bonds, to N1 (2.322(3) Å), Cl1 (2.352(1) Å, Cl2 (2.372(1) Å) for Hg1, and to N2 (2.316(3) Å), Cl3 (2.399(1) Å, Cl4 (2.319(1)Å) for Hg2. The coordination sphere of Hg1 and Hg2 is completed by Cl3 and Cl2, respectively, with dHg-Cl distances in the 2.757(6)–3.054(6) Å range, as observed for similar compounds forming square bridging systems [32, 33]. The range of angles around the Hg center [83.1(1)- 145.9(5)°] indicates that Hg presents $HgNCl_3$ coordination, distorted from ideal tetrahedral geometry. The metal centers are connected through two bridging chlorides to form Hg_2Cl_2 asymmetric lozenge rings with a distance between metal centers equivalent to 3.893(1) Å. The helical chain propagates along the c axis and has a pitch length of 17.35Å (Fig. 3b). Within a single stand, the ligand exhibits exclusively the right-handed *P* or the left-handed *M* conformation. The *P* and *M* helices are arranged alternately and linked through Hg—Cl···Cg interactions [$Cl1\cdots Cg4^{i}$ = 3.920(2) and $Cl4\cdots Cg2^{ii}$ = 3.753(2)] and the Hg—Cl···Cg angles are acute [$Hg—Cl1\cdots Cg4^{i}$ =83.14(4)° and $Hg—Cl4\cdots Cg2^{ii}$ = 84.93(4)°], Cg2 and Cg4 are the centroids of the N1/C1-C5 and C6-C11 rings, respectively [symmetry code : (i) x, 1+y, z ; (ii) 1-x, ½+y, ½-z]. Each helical chain shows the opposite helicity to the neighboring chain so that the whole complex $(HgCl_2)_2(\boldsymbol{L})$ is racemic (Fig. 3c).

Table 4: Selected experimental geometrical parameters (Å, °) of $(HgCl_2)_2(\boldsymbol{L})$, $(CoCl_2)_2(\boldsymbol{L})_2.CHCl_3$, and $Zn(SiF_6)(\boldsymbol{L})_2$

$(HgCl_2)_2(\boldsymbol{L})$			
Hg1—Cl1	2.351(1)	Hg2—Cl3	2.411(1)
Hg1—Cl2	2.382(1)	Hg2—Cl4	2.315(2)
Hg1—Cl3	2.841(1)	Hg2—Cl2	3.046(6)
Hg1—N1	2.315(3)	Hg2—N2^{i}	2.311(3)
N1—Hg1—Cl1	102.7(1)	N2—Hg2—Cl4^{i}	110.0(2)
N1—Hg1—Cl2	108.6(1)	N2—Hg2—Cl3^{i}	103.4(1)
Cl1—Hg1—Cl2	141.9(1)	Cl4—Hg2—Cl3	145.9(5)
N1—Hg1—Cl3	89.0(1)	N2—Hg2—Cl2^{i}	109.8(3)
Cl1—Hg1—Cl3	113.9(1)	Cl4—Hg2—Cl2	104.4(3)
Cl2—Hg1—Cl3	88.2(1)	Cl3—Hg2—Cl2	83.1(1)
Hg1—Cl2—Hg2	91.6(1)	Hg1—Cl3—Hg2	95.8(1)
Symmetry codes: (i) x, 1/2-y, -1/2+z			
$(CoCl_2)_2(\boldsymbol{L})_2.CHCl_3$			
Co1—N1	2.020(2)	Co1—Cl1	2.218 (1)
Co1—N2^{i}	2.038(2)	Co1—Cl2	2.230 (1)
N1—Co1—N2^{i}	104.81 (7)	N1—Co1—Cl2	109.18 (5)
N1—Co1—Cl1	112.18(5)	N2—Co1—Cl2	103.34(6)
N2—Co1—Cl1	109.94 (6)	Cl1—Co1—Cl2	116.42 (3)
Symmetry codes: (i) 1/2-x, 1/2-y, 2-z			
$Zn(SiF_6)(\boldsymbol{L})_2$			

Zn1—F1	2.089(2)	Si1—F1	1.720(2)
Zn1—F1^{i}	2.089(2)	Si1—F1^{ii}	1.720(2)
Zn1—N1	2.114(4)	Si1—F2	1.680(4)
Zn1—N1^{i}	2.114(4)	Si1—F3	1.675(2)
Zn1—N2	2.183(4)	Si1—F3^{ii}	1.675(2)
Zn1—N2^{i}	2.183(4)	Si1—F4	1.680(4)
F1—Zn1—F1^{i}	179.9(2)	F1—Si1—F1^{ii}	179.6(2)
F1—Zn1—N1	91.4(2)	F1—Si1—F2	89.8(1)
F1—Zn1—N1^{i}	88.6(2)	F1—Si1—F3	90.2(2)
F1—Zn1—N2	94.2(2)	F1—Si1—F4	90.2(2)
F1—Zn1—N2^{i}	85.8(2)	F1—Si1—F3^{ii}	89.8(2)
N1—Zn1—N2	90.0(2)	F2—Si1—F3	90.2(2)
N1—Zn1—N1^{i}	98.8(2)	F2—Si1—F3^{ii}	90.2(2)
N1—Zn1—N2^{i}	170.6(2)	F2—Si1—F4	180
N2—Zn1—N2^{i}	81.2(2)	F3—Si1—F4	89.8(2)
Zn1—F1—Si1	168.2(2)		

Symmetry codes: (i) ½-x, ½-y, z, (ii) 2-x, y, 1-z

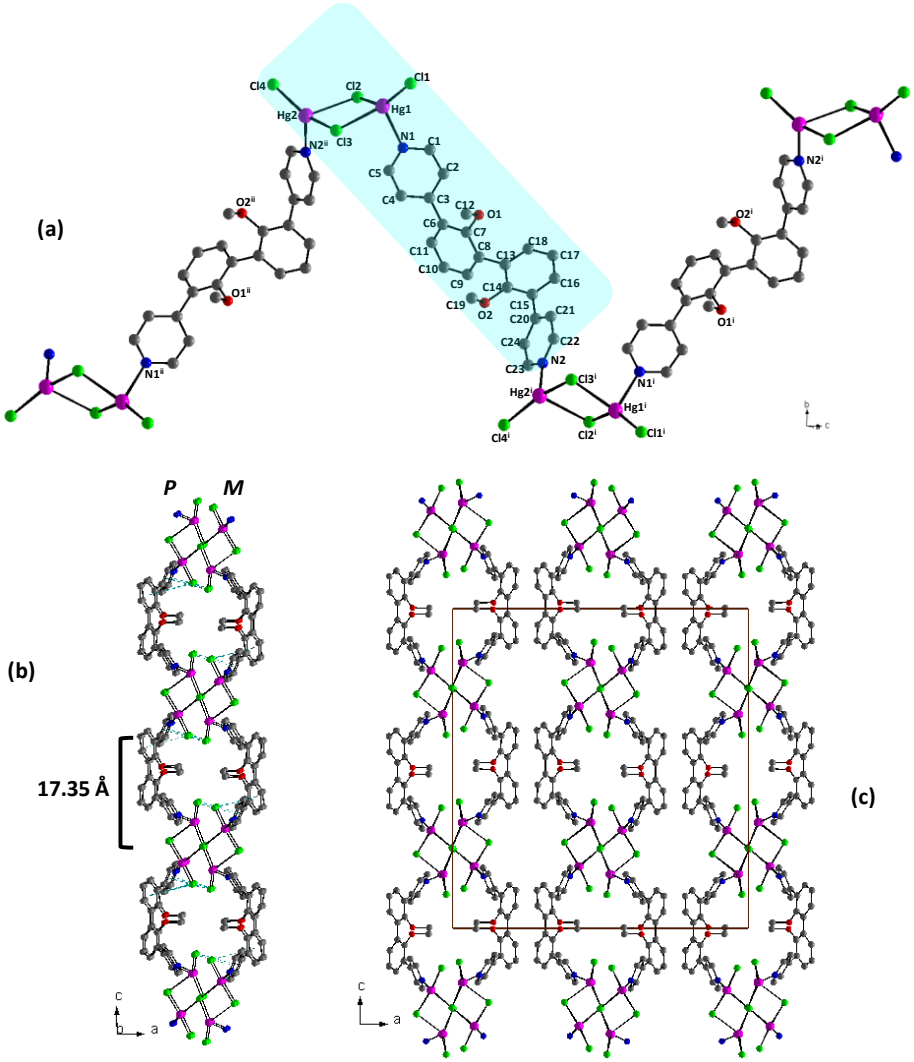

Figure 3: Crystal structure of $(HgCl_2)_2(\boldsymbol{L})$, (a) 1D chain of $(HgCl_2)_2(\boldsymbol{L})$. Hydrogen atoms are omitted for clarity. Symmetry code (i) x, ½-y, ½+z, (ii) x, ½-y, -½+z, (b) Side view of the helical chains and (c) packing diagram viewed along the b-axis

3.4. Crystal structure of $(CoCl_2)_2(\boldsymbol{L})_2.CHCl_3$

X-ray diffraction analyses show that the resulting complex $(CoCl_2)_2(\boldsymbol{L})_2.CHCl_3$ crystallizes in the monoclinic space group C2/c (Table 1). Selected bond lengths and bond angles are given in Table 4. Two ligands bridge two cobalt atoms through the terminal pyridinyl group, forming in a $Co_2\boldsymbol{L}_2$-type metallocyclic motif, while the two remaining sites are occupied by chloride ions with the Co···Co distance of 13.137(1) Å. The two opposite pyridine rings of the ligand spacer have a distance of 10.594 Å and 10.691 Å, respectively. Inside the macrocycle, a solvent molecule is connected through a bifurcated H-bond with two oxygen atoms of the ligands (Fig. 4a). The Co(II) ion is coordinated by two pyridyl nitrogen atoms [Co—$N_{pyridyl}$ distances

2.020(2) Å and 2.038(2) Å] and two chlorides [Co—Cl1 = 2.218 (1) and Co—Cl1 =2.230 (1) Å; the N—Co—N angle is 104.81(7)°], leading to a distorted tetrahedral geometry around Co(II). The two pyridine rings coordinating to the Co atom are perpendicular, making a dihedral angle of 89.1(2)° to each other. For the ligand, the dihedral angle between the pyridyl and the phenyl is equivalent to 43.9 and 48.5° respectively, whereas the two phenyl groups are tilted by 55.8°.

The analysis of the crystal packing reveals the presence of C—H···Cl (C···Cl distance 3.357 – 3.754 Å) (Fig. 4b and Table 3), C—H···π interactions occurring from the methyl to the benzene ring (C6-C11) (Fig 4c). In addition, the conformation of the metallocycles is stabilized by π···π stacking interactions between benzene (C6-C11), and pyridine (N1/C1-C5) rings [centroid-centroid distance 3.912(1) Å] (Fig. 4d), forming a 3D supramolecular structure (Fig. 4e).

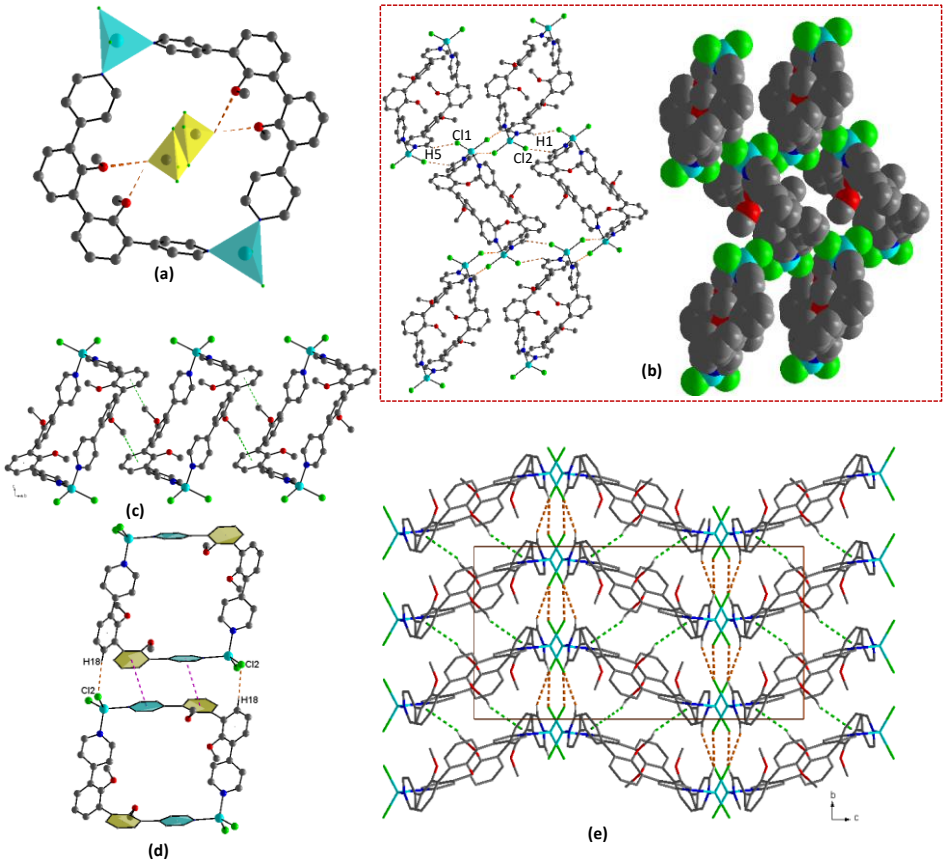

Figure 4: (a) picture of the centro-symmetric dimeric unit of $Co_2Cl_4(\boldsymbol{L})_2.CHCl_3$. (b) C—H···Cl hydrogen bond interactions, (c) view a C—H···π stacking leading to the formation dimeric along the b-axis, (d) π···π stacking interaction forming 1D chain along the c-axis and (e) packing crystal viewed along the a-axis respectively. Hydrogen atoms and solvent molecules are omitted for clarity.

3.5. Crystal structure of $Zn(SiF_6)(\boldsymbol{L})_2$.

Compound $Zn(SiF_6)(\boldsymbol{L})_2$ crystallizes in the orthorhombic system with non-centrosymmetric space group *C*222 (Table 1), containing half a Zn^{2+} cation, one organic ligand, and half a SiF_6^{2-} anion in its asymmetric unit (Fig. 5a). Selected bond lengths and bond angles are given in Table 4. The coordination sphere around the metal center is composed of two F atoms (Zn–F distance in the 2.09 Å range) and four N atoms belonging to four organic ligand ***L*** (Zn–N distance in the 2.11–2.19 Å range). While, the coordination geometry around the Si atoms is a distorted octahedron with two sets of Si–F bonds (Si–F distance in the range of 1.67–1.69 Å and 1.72 Å for F atoms located at the square base and two occupying the apical positions, respectively). SiF_6^{2-} anions were found to bridge two metal centers with a Zn—Zn distance of 7.725 Å. As expected and according to the previous observation with reported structures [34, 35], the octahedral zinc and octahedral SiF_6^{2-} lead to the formation of an infinite chain through mutual bridging between the two species. Therefore, in our complex the interconnection of $ZnSiF_6$ pillars by the ligand is along the diagonal.

The four ligands around each Zn cation adopt a distorted zigzag shape to form a plane, as shown in Figure 5b. Two consecutive planes are bridged by the SiF_6^{2-} leading to a 3D supramolecular structure with channels along an a-axis controlled by the organic ligand which, imposes the distances (Fig. 5d). The potential solvent-accessible volume calculated using the *Platon software* [36] is 2528.1Å^3, corresponding to 40.7% of the total unit cell volume for $Zn(SiF_6)(\boldsymbol{L})_2$ (6208.3 Å^3).

For the ligand ***L***, the dihedral angle between two pyridine rings giving a value of 49.8(2)°, while the two pyridine rings coordinating to the Zn atom are nearly perpendicular, making a dihedral angle of 83.4(2)°. Moreover, Tthe structure is stabilized by C—H···O and C—H···F hydrogen bonds (Table 3) to form a 3D supramolecular structure. This framework is reinforced by both C—H···π interactions (Fig. 5c-d).

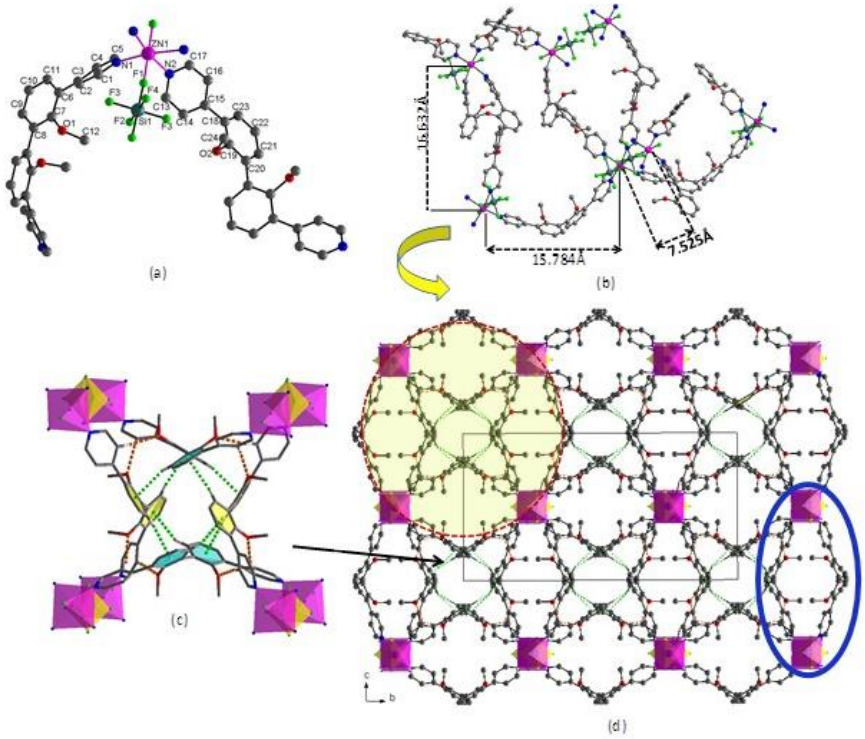

Figure 5: Crystal structure of the complex $Zn(SiF_6)(\boldsymbol{L})_2$, (a) coordination sphere around Zn(II) metal, (b) view of neighboring plane along the direction of $ZnSiF_6$, (c) C—H···O interactions bonds and C—H···π interactions and (d) packing diagram along a-axis with kinds of pore. Hydrogen atoms have been omitted for clarity.

As mentioned earlier, $Zn(SiF_6)(\boldsymbol{L})_2$ crystallizes in a chiral space group (orthorhombic system, *C*222). The Flack parameter determined for the resolved structure is calculated tobe 0.004(19). In this structure, the chirality arises from the helicity drawn by the arrangement of the ***L*** ligands along with the infinite $Zn(SiF_6)$ linear chains (Figure 6). More precisely, for the analyzed crystal the helical descriptor is *P*.

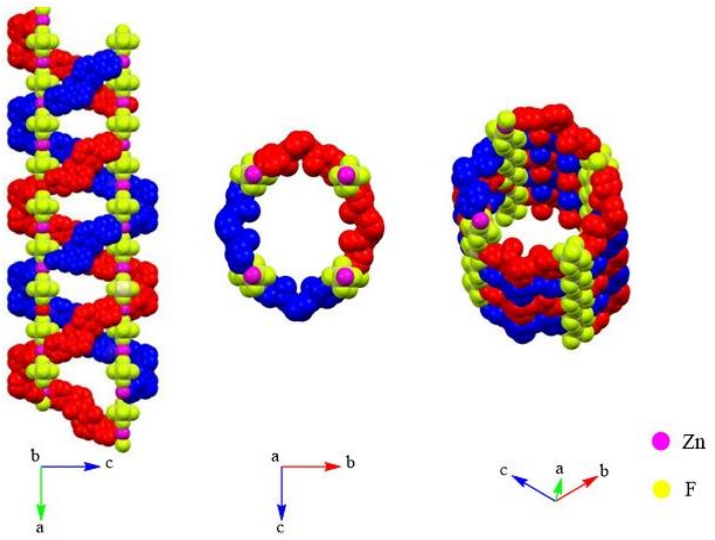

Figure 6: Portion of the X-ray structure of showing the double stranded helical repeating motifs in different views. This view corresponds to the region of the networks encircled in red in Figure 5. The **L** ligands are in two colours (red and blue) to better visualize the *P* helicity of the assembly. Hydrogen atoms have been omitted for clarity.

4. Conclusion

In this work the synthesis of novel $(HgCl_2)_2(\boldsymbol{L})$, $(CoCl_2)_2(\boldsymbol{L})_2.CHCl_3$ and $Zn(SiF_6)(\boldsymbol{L})_2$ based on mixed ligands ***L*** (3,3'-di(pyridin-4-yl)-(2,2'-dimethoxy-[1,1'-biphenyl]) and $HgCl_2$, $CoCl_2$ or $ZnSiF_6$ have been rationally prepared. A single crystal X-ray structural analysis shows that the compounds crystallize in the *P*bca, *C*2/c and *C*222 space groups, respectively. Two helical infinite networks with opposite chirality (*P* and *M*) were characterized for $(HgCl_2)_2(\boldsymbol{L})$and are helical tubular assemblies of the **L** ligands attached to two $Zn(SiF_6)_\infty$ pillars for $Zn(SiF_6)(\boldsymbol{L})_2$.The combination of Co(II) with **L** forms a metallo-macrocycle.

The current work illustrates that the 2,2'-dimethoxy-1,1'-biphenyl framework within a ligand are intriguing ligand for construction of unprecedented helical coordination compounds and our efforts are now continuously dedicated to develop stereoselective approaches to create enantiopure helical CPs analogous ligands to explore different architectures and topologies.

Supplementary material

These data include NMR spectra for ***L***. CCDC n°: 2064620, 2064622, 2064624 and 2064623 contain the supplementary crystallographic data for compound ***L***, $(HgCl_2)_2(\boldsymbol{L})$, $(CoCl_2)_2(\boldsymbol{L})_2.CHCl_3$ and $Zn(SiF_6)(\boldsymbol{L})_2$, respectively. These data can be obtained free of charge via www.ccdc.cam.ac.uk/data_request/cif, or by emailing data_request@ccdc.cam. ac.uk, or by

contacting the Cambridge Crystallographic Data Centre, 12 Union Road, Cambridge CB2 1EZ, UK; fax: + 44 1223 336033.

Acknowledgements

This work was financial supported by the University of Strasbourg and CNRS.

References

[1] J. L. Bada, Nature 374 (1995) 594-595.
[2] C. Janiak, Dalton Trans. (2003) 2781-2804.
[3] S. Wang, D. Bai, Y. Wang, J. Fu, J. Zhu, X. Fang, 12, *Nanoscale* (2020) 10972-10976.
[4] Y. Liu, W. Li, Y. -Q. Yang, M. -S. Chen W. -W. Fu, J. Struct. Chem. 62 (2021) 740–747.
[5] S. E. H. Etaiw, Safaa N. Abdou, J. Inorg Organomet Polym. 26 (2016) 117–126.
[6] E. Yashima, N. Ousaka, D. Taura, K. Shimomura, T. Ikai, K. Maeda Chem. Rev. 116 (2016) 13752-13990.
[7] A. Ebina, S. Hossain, H. Horihata, S. Ozaki, S. Kato, T. Kawawaki, Y. Negishi, Nanomaterials 10 (2020) 1105.
[8] S. Henfling, O. A. Saputra, H. Krautscheid, Z. Anorg. Allg. Chem. 647 (2021) 1–9.
[9] S. E. H. Etaiw, H. Marie, E. M. Shalaby, R. S. Farag, F. A. Elsharqawy, Appl. Organometal Chem. 33 (2019) e5114.
[10] C. E. Housecroft E. C. Constable, Chem. Commun. 56 (2020) 10786-10794.
[11] K. Nishinaka, J. Han, D. Han, Y. Liu, Y. Du, M. Wang, C. Eerdun, N. Naruse, Y. Mera, Y. Furusho, A. Tsuda, Front. Chem. 8 (2020) 613932.
[12] L. Carlucci, G. Ciani and D. M. Proserpio, Coord. Chem. Rev. 246 (2003) 247-289.
[13] G. Férey, C. Mellot-Draznieks, C. Serre, F. Millange, Acc. Chem. Res. 38 (2005) 217-225.
[14] S. Kitagawa and K. Uemura, Chem. Soc. Rev. 34 (2005) 109-119.
[15] D. Maspoch, D. Ruiz-Molina and J. Veciana, Chem. Soc. Rev. 36 (2007) 770-818.
[16] J. R. Long and O. M. Yaghi, Chem. Soc. Rev. 38 (2009) 1213-2114.
[17] M. Yoon, R. Srirambalaji and K. Kim, Chem. Rev. 112 (2012) 1196-1231.
[18] Y. Shi, A-F. Yang, C-S. Cao, B. Zhao, Coord. Chem. Rev. 390 (2019) 50-75.
[19] S. E. H. Etaiw, H. Marie, Sens. Actuators B Chem. 290 (2019) 631–639.
[20] S. E. H. Etaiw, T. A. Fayed | M. M. El - bendary, H. Marie, J. Inorg. Organomet. Polym. Mater. 28 (2018)508–518.
[21] P. Wang , Y. Sun, X. Li, L. Wang, Y. Xu, G. Li, Molecules 26 (2021) 209-226.
[22] P. Silva, S. M. F. Vilela, J. P. C. Tomé, F. A. Almeida Paz, Chem. Soc. Rev. 44 (2015) 6774-6803.
[23] Y. Fang, W-M. Xuan, C-F. Zhu, G-Z. Yuan, Y. Cui, Chinese J. Struct. Chem. 30 (2011) 1147-1153.
[24] G. Yuan, C. Zhu, Y. Liu, W. Xuan, Y. Cui, J. Am. Chem. Soc. 131 (2009) 10452-10460.
[25] A. Jouaiti, M. W. Hosseini, N. Kyritsakas, P. Grosshans, J-M. Planeix, Chem. Comm. 29 (2006) 3078-3080.
[26] P. Mobian, C. Huguenard M. Henry, Chem. Comm. 47 (2011) 9630-9632.
[27] A. Kayal, A.F. Ducruet, S.C Lee, Inorg. Chem. 39 (2000) 3696-3704.
[28] Bruker, APEX3 (Version 5.054), SAINT + (Version 6.36A), SADABS, Bruker AXS Inc., Madison, Wisconsin, USA, 2016.
[29] G.M. Sheldrick , Acta Crystallogr. Sect. A Found. Crystallogr. 71 (2015) 3-8.
[30] G.M. Sheldrick , Acta Crystallogr. Sect. C Struct. Chem. 71 (2015) 3-8.

[31] K. Brandenburg, DIAMOND, Crystal Impact GbR, B Bonn, Germany, 2006.
[32] M. Guerrero, J. Pons, J. Ros, M. F.-Bardia, O. Vallcorba, J. Rius, V. Branchadelld, A. Merkoc, CrystEngComm. 13 (2011) 6457-6470
[33] Rodrigo S. Bitzer, Lorenzo C. Visentin, Manfredo Hörner, Marco A. C. Nascimento, Carlos A. L. Filgueiras, J. Coord. Chem. 70 (2017) 1089-1104.
[34] M-J. Lin, A. Jouaiti, N. Kyritsakas and M. W. Hosseini, Molecular tectonics: control of interpretation in cuboid 3-D coordination networks, *CrystEngComm*. 13 (2011) 776-778.
[35] P. Larpent, A. Jouaiti, N. Kyritsakas and M. W. Hosseini, Chem. Comm. 49 (2013) 4468-4470.
[36] A. L. Spek, *Platon*, the University of Utrecht, Utrecht, the Netherlands, 1999